IOSR Journal of Mechanical and Civil Engineering (IOSR-JMCE)
e-ISSN: 2278-1684,p-ISSN: 2320-334X, Volume 15, Issue 1 Ver. IV (Jan. - Feb. 2018), PP 44-56
www.iosrjournals.org

Numerical simulation of compressible viscous flow

Nacer E. EL KADRI E.
Sidi Mohamed Ben Abdellah University, Department of Mathematics Physics and Informatics, Polydisciplinary Faculty, Laboratory - LSI, P.O. Box 1223 , Taza, Morocco.

Abstract: *The purpose of this research is the study and improvement of numerical methods to solve viscous compressible flows. The equations represent these flows are solved in the conservative form with a comparison between conservative variables and new variables called pseudo-primitive variables. The discretization in space is performed by the finite element method and the discretization in time is accomplished by a finite difference method. Among the objectives of this work is the simulation of dominant convective flows, the case where the Reynolds number and the Mach number are high. Knowing that when advection flows dominate diffusion flows, the discretization of advection-diffusion equations by Galerkin's standard finite element method presents non-physical oscillations, which makes the method unstable. To stabilize the solutions a variant of the finite element method of Petrov-Galerkin is developed. The nonlinear system resulting from the discretization is solved by the iterative algorithm GMRES with a diagonal pre-conditioning. Various simulations, ranging from transonic flows to supersonic flows are treated, for the systematic validation of the methods and techniques developed.*

Keywords - *Advection-diffusion, Compressible Viscous Flow, Finite element, GMRES, Petrov-Galerkin.*

Date of Submission: 06-02-2018 Date of acceptance: 24-02-2018

I. Introduction

This research contributes to the study and improvement of numerical methods for the simulation of viscous compressible flows. These flows are described by the Navier-Stokes equations. To solve these equations numerically, a first step is to choose the form of these equations and the independent variables to use. Indeed, there are several possible choices, mainly: the conservative form [1-4], the conservative form using the entropic variables [5], and the non-conservative form [6, 7]. A priori, the conservative form is the most suitable, both physically and numerically, especially for shock wave flows. This is because the conservation equations are solved as derived from conservation laws. Moreover, this form directly expresses the variables that are naturally conserved through discontinuities. In this work, the Navier-Stokes equations are solved in the conservative form using two types of independent variables: conservative variables (density, momentum per unit volume and total energy per unit volume), and pseudo-primitive variables (static pressure, momentum per unit volume and temperature). This study was carried out in order to represent as precisely as possible the physical and natural boundary conditions, to satisfy the second principle of thermodynamics and finally to develop a general conservation form able to use any type of independent variables.

Knowing that when advection flows dominate diffusion flows, the discretization of advection-diffusion equations by Galerkin's standard finite element method presents non-physical oscillations, which makes the method unstable. These oscillations are due to the negative numerical diffusion produced by Galerkin's standard finite element method [8]. Stabilization methods have been used for problems dominated by advection to suppress oscillations and improve the stability of the numerical solution. In Computational Fluid Dynamic (CFD), the common remedy is to add a numerical dissipation. Several stabilization methods have been developed, Streamline Upwind Petrov-Galerkin (SUPG) is one of the popular stabilization methods for advection dominated problems [9-13], in fixed areas. Other stabilization methods such as Galerkin Least-Squares (GLS) [14], edge stabilization [15], continuous interior penalty [16], local projection stabilization [17] orthogonal sub-grid scale [18] and Variational Multi-Scale (VMS) [19-21] have also been proposed in the literature for fixed domains, for an overview see [22]. A comparison of the SUPG method with other stabilization methods for a problem in a fixed domain can be found in [8]. An adaptive SUPG method for a transient problem in a fixed domain has been analyzed in [23]. In [24], a comparative study of different SUPG stabilization parameters was performed. A detailed study of the stabilization methods for compressible flows, including their formulation and history, can be found in [13].

We use triangular elements for which the components of velocity and momentum per unit volume are approximated by continuous polynomials of the second degree whereas the other variables are approximated by continuous linear polynomials. This choice of mixed polynomial approximations makes it possible to check the stability of the element, satisfying the "Inf-Sup" condition [25, 26]. The nonlinear system resulting from the discretization is solved by the iterative GMRES algorithm with diagonal preconditioning [27, 28]. Various test cases, ranging from transonic flows to supersonic flows, are treated for the systematic validation of the methods and techniques developed.

II. Mathematical formulation

In this section, we present the equations of fluid dynamics; to solve numerically these equations the first step is the choice of a form and independent variables.

II.1. Equations of fluid dynamics

The equations of fluid dynamics result from conservation laws: conservation of mass, conservation of moment (Newton's second law) and conservation of energy (first and second laws of thermodynamics). To write these equations, the concept of total derivative, the Reynolds transport theorem and the Gaussian theorem are used. Let Ω be a bounded domain of $\mathbb{R}^n$ and Γ its boundary (in practice we take $n = 1, 2$ or 3).

- Conservation of mass - the continuity equation

$$\frac{\partial \rho}{\partial t} + \nabla \cdot (\rho \mathbf{u}) = 0 \tag{1}$$

- Conservation of momentum

$$\frac{\partial \rho \mathbf{u}}{\partial t} + \nabla \cdot (\rho \mathbf{u} \otimes \mathbf{u}) + \nabla p = \nabla \cdot \underline{\sigma} + \rho \mathbf{f} \tag{2}$$

- Conservation of energy

$$\frac{\partial \rho e}{\partial t} + \nabla \cdot [(\rho e + p)\mathbf{u}] = \nabla \cdot \left(\underline{\sigma} \cdot \mathbf{u}\right) - \nabla \cdot \mathbf{q} + \rho \mathbf{f} \cdot \mathbf{u} \tag{3}$$

In the above relations, ρ is the density, $\mathbf{u}$ is the velocity, p is the pressure, $\underline{\sigma}$ is the viscous stress tensor, $\mathbf{f}$ is the body force, e is the total specific energy ($e = i + \frac{1}{2}|\mathbf{u}|^2$) and $\mathbf{q}$ is the heat flux. The fluid is isotropic and Newtonian, the viscous stress tensor $\underline{\sigma}$ is given by:

$$\underline{\sigma} = -\frac{2}{3}\mu(\nabla \cdot \mathbf{u})\underline{I} + \mu[\nabla \mathbf{u} + (\nabla \mathbf{u})^t] \tag{4}$$

where μ is the dynamic viscosity. The heat flux $\mathbf{q}$ is given by Fourier's law:

$$\mathbf{q} = -\lambda \nabla T \tag{5}$$

where λ is the thermal conductivity and T is the temperature. In the case of two-dimensional flows, we have only four equations to determine the five unknown variables$(\rho, u_1, u_2, p$ and $T)$, in the case where the transport coefficients (thermal conductivity λ and μ dynamic viscosity) are expressed in terms of these five unknown variables. In the case of a compressible fluid such as air, the ideal gas law can be used:

$$p = \rho R T \tag{6}$$

where $R = c_p - c_v$ is the gas constant. The quantities c_v and c_p are respectively the specific heat at constant volume and the specific heat at constant pressure.

II.2. Forms of the equations of conservation

To solve numerically the equations of mass conservation, momentum conservation and energy conservation, we must choose the form of these equations and the independent variables to be used. Indeed, there are several possible choices, mainly:

- The non-conservation form [6, 7] where the conservation equations (1, 2 and 3) are transformed in order to simplify them and to show the appropriate independent variables ($(p, u_1, u_2$ and $T)$ for example). To obtain the non-conservative form, the system of equations (1, 2 and 3) is transformed in order to write it according to the independent variables and their variations. Mathematically, the transformations performed on these equations are not valid in the presence of a surface of discontinuity, since neither velocity, density nor certain other quantities are continuous. Consequently, in the presence of a discontinuity surface, equations of the non-conservation form are not equivalent to the original equations (1, 2 and 3). The choice of this form can be justified given that the physical and natural boundary conditions on temperature and velocity are represented as accurately as possible.

- The conservation form in entropic variables [5] where the conservation equations (1, 2 and 3) are expressed in terms of the so-called entropic variables $\frac{1}{T}\left(\frac{-|\mathbf{u}|^2}{2} + \gamma T - Ts, \mathbf{u}, -1\right)$. The conservation form in entropic variables is characterized by two important properties. The first property is that this form leads to a system of advection-diffusion equations where all matrices are symmetric. The second property is that with this form the second principle of thermodynamics is directly satisfied. This form allowed to develop the first upwind finite element method for compressible fluids, this method is known as Streamline Upwind Petrov-Galerkin (SUPG). However, such a form does not make it easy to apply physical boundary conditions because of the type of independent variables used.

- The conservation form [1-4] where the conservation equations, (1, 2 and 3) are directly considered without any transformation. This form expresses directly the variables that are naturally conserved through discontinuities. Numerically, the conservation form is best adapted because problems of fluid dynamics often present areas of discontinuities. Physically, the conservation form is best adapted because the fluid dynamics equations are solved by perfectly respecting the laws of physics; in addition the boundary conditions are directly imposed on the physical variables.

By this work our contribution consists of solving problems of fluid dynamics at high Reynolds and Mach numbers. Thus, the Navier-Stokes equations are studied in conservation form. In order to apply the boundary conditions as accurately as possible, different types of independent variables were used while keeping the conservation form. In the following, we present the conservation equations in the conservation form and we define the conservative variables. The conservation form will be generalized in order to use any types of independent variables.

II.3. Conservative form in conservative variables

In order to determine the conservation form in conservative variables, the conservative variables: the density ρ, the momentum per unit volume $\mathbf{U}$ and the total energy per unit volume E are directly taken as independent variables in the conservation equations (1, 2 and 3). Thus, the conservative form in conservative variables of the conservation equations (1, 2 and 3) are written as follows:

- Equation of mass conservation:

$$\frac{\partial \rho}{\partial t} + \nabla \cdot \mathbf{U} = 0 \tag{7}$$

- Equation of the conservation of momentum:

$$\frac{\partial \mathbf{U}}{\partial t} + \nabla \cdot (\mathbf{U} \otimes \mathbf{u}) + \nabla p = \nabla \cdot \underline{\sigma} + \rho \mathbf{f} \tag{8}$$

- Equation of conservation of energy:

$$\frac{\partial E}{\partial t} + \nabla \cdot [(E + p)\mathbf{u}] = \nabla \cdot \left(\underline{\sigma} \cdot \mathbf{u}\right) - \nabla \cdot \mathbf{q} + \mathbf{f} \cdot \mathbf{U} \tag{9}$$

The flow velocity and the temperature, as a function of the conservative variables, are expressed respectively by the following relations:

$$\mathbf{u} = \frac{\mathbf{U}}{\rho} \tag{10}$$

$$E = \rho e = \rho \left[c_v T + \frac{|\mathbf{U}|^2}{2\rho^2}\right] \quad \Longrightarrow \quad T = \frac{1}{c_v}\left[\frac{E}{\rho} - \frac{|\mathbf{U}|^2}{2\rho^2}\right] \tag{11}$$

To express the pressure and the heat flux as a function of the conservative variables $(\rho, \mathbf{U}, E)$, equation (11) is combined with the ideal gas law (6) and the Fourier law (5). Thus, the following relations are obtained:

$$p = (\gamma - 1)\left[E - \frac{|\mathbf{U}|^2}{2\rho^2}\right] \tag{12}$$

$$\mathbf{q} = -\frac{\lambda}{c_v}\nabla\left[\frac{E}{\rho} - \frac{|\mathbf{U}|^2}{2\rho^2}\right] \tag{13}$$

To express the viscous stress tensor according to conservative variables, equation (10) is combined with equation (4). Thus, the viscous stress tensor, as a function of the conservative variables, is written as follows:

$$\underline{\sigma} = \frac{\mu}{\rho}\left[\nabla\mathbf{U} + (\nabla\mathbf{U})^t - \frac{2}{3}(\nabla\cdot\mathbf{U})\underline{I}\right] + \underline{\sigma}^{\ddagger} \tag{14}$$

where

$$\underline{\sigma}^{\ddagger} = -\frac{\mu}{\rho^2}\left[\mathbf{U}\cdot(\nabla\rho)^t + (\nabla\rho)\cdot\mathbf{U}^t - \frac{2}{3}(\mathbf{U}^t\cdot\nabla\rho)\underline{I}\right]$$

In the following subsection, we introduce a new type of independent variables, we will develop the conservative form in pseudo-primitive variables.

II.4. Conservative form in pseudo-primitive variables

The conservation form in pseudo-primitive variables uses the independent variables $\mathbf{Y} = (p, \mathbf{U}, T)^t$. To obtain the conservation form in pseudo-primitive variables, the equations (1, 2 and 3) are transformed in order to express them in terms of the independent variables and their derivatives. In this form, the density ρ is expressed as a function of the pseudo-primitive variables $(p, \mathbf{U}, T)$, using the ideal gas law

$$\rho = \frac{p}{RT} \tag{15}$$

The time derivative of the density ρ is given by:

$$\frac{\partial\rho}{\partial t} = \frac{1}{RT}\frac{\partial p}{\partial t} - \frac{p}{RT^2}\frac{\partial T}{\partial t} \tag{16}$$

The conservative form in pseudo-primitive variables is written as follows:

- Equation of mass conservation:

$$\left(\frac{1}{RT}\right)\frac{\partial p}{\partial t} - \left(\frac{p}{RT^2}\right)\frac{\partial T}{\partial t} + \nabla\cdot\mathbf{U} = 0 \tag{17}$$

- Equation of the conservation of momentum:

$$\frac{\partial\mathbf{U}}{\partial t} + \nabla\cdot(\mathbf{U}\otimes\mathbf{u}) + \nabla p = \nabla\cdot\underline{\sigma} + \frac{p}{RT}\mathbf{f} \tag{18}$$

- Equation of conservation of energy:

$$\frac{\partial\rho i}{\partial t} + \frac{\partial\rho e_c}{\partial t} + \nabla\cdot[(\rho i + \rho e_c + p)\mathbf{u}] = \nabla\cdot\left(\underline{\sigma}\cdot\mathbf{u}\right) - \nabla\cdot\mathbf{q} + \mathbf{f}\cdot\mathbf{U} \tag{19}$$

or :

$$\left(\frac{|\mathbf{U}|^2R}{2p}\right)\frac{\partial T}{\partial t} + \left(\frac{1}{\tilde{\gamma}} - \frac{|\mathbf{U}|^2RT}{2p^2}\right)\frac{\partial p}{\partial t} + \left(\frac{U_1RT}{p}\right)\frac{\partial U_1}{\partial t} + \left(\frac{U_2RT}{p}\right)\frac{\partial U_2}{\partial t}$$
$$+\nabla\cdot\left[\left(c_pT + \frac{|\mathbf{U}|^2R^2T^2}{2p^2}\right)\mathbf{U}\right] = \nabla\cdot\left(\underline{\sigma}\cdot\mathbf{u}\right) - \nabla\cdot\mathbf{q} + \mathbf{f}\cdot\mathbf{U}$$

with

$$\tilde{\gamma} = \gamma - 1 \quad \text{and} \quad e_c = \frac{|\mathbf{u}|^2}{2}$$

The velocity $\mathbf{u}$ is calculated as a function of the pseudo-primitive variables, using the expressions of the density (15) and the momentum per unit volume:

$$\mathbf{u} = \frac{\mathbf{U}RT}{p} \tag{20}$$

The heat flux is given by the Fourier law (5). The viscous stress tensor is evaluated by equation (4) where the velocity is calculated by the relation (20). In the system of equations (17, 18 and 19), the equation of mass conservation is considered the pressure equation, the equation of the conservation of the momentum is considered the equation of the momentum per unit of volume and the equation of energy conservation is considered the equation of temperature.

II.5. Generalization of conservative form

The conservation form in conservative variables (7, 8 and 9) can be written in the vector form:

$$\mathbf{V}_{,t} + \mathbf{F}_{i,i}^{adv}(\mathbf{V}) = \mathbf{F}_{i,i}^{diff}(\mathbf{V}) + \boldsymbol{\mathcal{F}} \tag{21}$$

Where $\mathbf{V} = (\rho, \mathbf{U}, E)^t$ is the vector of the conservative variables, $\mathbf{F}_i^{adv}$ is the advection flux in the i direction, $\mathbf{F}_i^{diff}$ is the diffusion flux in the same direction and $\boldsymbol{\mathcal{F}}$ is the source vector. The system of equations (21) in the quasi-linear form [29, 30] is written:

$$\mathbf{V}_{,t} + \mathbf{A}_i \mathbf{V}_{,i} = \left(\mathbf{K}_{ij}\mathbf{V}_{,j}\right)_{,i} + \boldsymbol{\mathcal{F}} \tag{22}$$

Where $\mathbf{A}_i$ are the Jacobian matrices of advection fluxes such that $\mathbf{A}_i = \mathbf{F}_{i,\mathbf{V}}^{adv}$, $\mathbf{K} = \left[\mathbf{K}_{ij}\right]$ are the diffusion matrices such that:

$$\mathbf{K}_{ij}\mathbf{V}_{,j} = \mathbf{F}_i^{diff}$$

In order to obtain a general conservation form, able to use any type of independent variables, the system (21) is transformed using the change of variables $\mathbf{V} = \mathbf{V}(\mathbf{Y})$. We obtain:

$$\mathbf{A}_0\mathbf{Y}_{,t} + \tilde{\mathbf{F}}_{i,i}^{adv}(\mathbf{Y}) = \tilde{\mathbf{F}}_{i,i}^{diff}(\mathbf{Y}) + \tilde{\boldsymbol{\mathcal{F}}} \tag{23}$$

with

$$\mathbf{A}_0 = \mathbf{V}_{,\mathbf{Y}} \qquad \mathbf{A}_0\mathbf{Y}_{,t} = \mathbf{V}_{,t} \qquad \text{and} \qquad \mathbf{A}_0\mathbf{Y}_{,i} = \mathbf{V}_{,i}$$

on the other hand :

$$\tilde{\mathbf{F}}_i^{adv}(\mathbf{Y}) = \mathbf{F}_i^{adv}(\mathbf{V}) \qquad \tilde{\mathbf{F}}_i^{diff}(\mathbf{Y}) = \mathbf{F}_i^{diff}(\mathbf{V}) \quad \text{et} \quad \tilde{\boldsymbol{\mathcal{F}}}(\mathbf{Y}) = \boldsymbol{\mathcal{F}}(\mathbf{V})$$

Where $\mathbf{A}_0$ represents the transformation matrix of the vector of the conservative variables $\mathbf{V}$ to the vector of other types of independent variables $\mathbf{Y}$. Thus, the system (22) becomes:

$$\mathbf{A}_0\mathbf{Y}_{,t} + \tilde{\mathbf{A}}_i\mathbf{Y}_{,i} = \left(\tilde{\mathbf{K}}_{ij}\mathbf{Y}_{,j}\right)_{,i} + \tilde{\boldsymbol{\mathcal{F}}} \tag{24}$$

with :

$$\tilde{\mathbf{A}}_i = \tilde{\mathbf{F}}_{i,\mathbf{Y}}^{adv} = \mathbf{A}_i\mathbf{A}_0 \qquad \text{and} \qquad \tilde{\mathbf{K}}_{ij} = \mathbf{K}_{ij}\mathbf{A}_0$$

If $\mathbf{Y} = \mathbf{V}$ the transformation matrix $\mathbf{A}_0$ then equals the identity matrix, so we find the conservation form in conservative variables.

III. Finite Element Formulation

In this work, the Navier-Stokes equations are solved by the finite element method for discretization in space and the finite difference method for discretization in time. In order to stabilize the solutions of the dominant advection problems, we use a variant of the Petrov-Galerkin finite element method. With this method we modify the Galerkin's standard finite elements method by adding to it a disturbance term of type upwind acting only in the direction of the flow and not transversally.

III.1. Space discretization

The weak variational formulation of conservative form in conservative variables (21) is given by:

$$\begin{aligned}
&\int_{\boldsymbol{\Omega}} \left\{\mathbf{W}\cdot\left[\mathbf{V}_{,t} + \mathbf{F}_{i,i}^{adv}(\mathbf{V}) - \boldsymbol{\mathcal{F}}\right] + \mathbf{W}_{,i}\cdot\left[\mathbf{F}_i^{diff}(\mathbf{V})\right]\right\}\mathrm{d}\boldsymbol{\Omega} \\
&+\sum_e \int_{\Omega^e} \left\{\left(\mathbf{A}_i^t\cdot\mathbf{W}_{,i}\right)\underline{\tau}\left[\mathbf{V}_{,t} + \mathbf{F}_{i,i}^{adv}(\mathbf{V}) - \mathbf{F}_{i,i}^{diff}(\mathbf{V}) - \boldsymbol{\mathcal{F}}\right]\right\}\mathrm{d}\Omega^e \\
&= \int_\Gamma \left\{\mathbf{W}\cdot\left[\mathbf{F}_i^{diff}(\mathbf{V})\cdot\mathbf{n}_i\right]\right\}\mathrm{d}\Gamma
\end{aligned} \tag{25}$$

where Ω^e is an element of the triangularization of Ω. In the quasi-linear form, the weak variational formulation is given by:

$$\begin{aligned}
&\int_{\boldsymbol{\Omega}} \left\{\mathbf{W}\cdot\left[\mathbf{V}_{,t} + \mathbf{A}_i\mathbf{V}_{,i} - \boldsymbol{\mathcal{F}}\right] + \mathbf{W}_{,i}\cdot\left[\mathbf{K}_{ij}\mathbf{V}_{,j}\right]\right\}\mathrm{d}\boldsymbol{\Omega} \\
&+\sum_e \int_{\Omega^e} \left\{\left(\mathbf{A}_i^t\cdot\mathbf{W}_{,i}\right)\underline{\tau}\left[\mathbf{V}_{,t} + \mathbf{A}_i\mathbf{V}_{,i} - \left(\mathbf{K}_{ij}\mathbf{V}_{,j}\right)_{,i} - \boldsymbol{\mathcal{F}}\right]\right\}\mathrm{d}\Omega^e \\
&= \oint_\Gamma \left\{\mathbf{W}\cdot\left[\left(\mathbf{K}_{ij}\mathbf{V}_{,j}\right)\cdot\mathbf{n}_i\right]\right\}\mathrm{d}\Gamma
\end{aligned} \tag{26}$$

This variational formulation is characterized by two important properties; it is a method of weighted residue and with a good choice of the matrix of stabilization $\underline{\tau}$, stability is improved thanks to the elliptic term:

$$\sum_e \int_{\Omega^e} \left\{ \left(\mathbf{A}_i^t \cdot \mathbf{W}_{,i} \right) \underline{\tau} \left(\mathbf{A}_i \mathbf{V}_{,i} \right) \right\} \mathrm{d}\Omega^e \tag{29}$$

The stabilization matrix $\underline{\tau}$ for the variational formulation of the conservative form in conservative variables [31 to 34], is written as follows:

$$\underline{\tau} = \left[\sum_i \left| c_{ij} \mathbf{A}_j \right| \right]^{-1} \zeta(Pe) \tag{30}$$

To obtain a general weak variational formulation, able to use any type of independent variables $\mathbf{Y}$, we replace the weak variational formulation (25) by:

$$\begin{aligned} &\int_{\mathbf{\Omega}} \left\{ \mathbf{W} \cdot \left[\mathbf{A}_0 \mathbf{Y}_{,t} + \tilde{\mathbf{F}}_{i,i}^{adv}(\mathbf{Y}) - \tilde{\boldsymbol{\mathcal{F}}} \right] + \mathbf{W}_{,i} \cdot \left[\mathbf{F}_i^{diff}(\mathbf{V}) \right] \right\} \mathrm{d}\mathbf{\Omega} \\ &+ \sum_e \int_{\Omega^e} \left\{ \left(\tilde{\mathbf{A}}_i^t \cdot \mathbf{W}_{,i} \right) \underline{\tilde{\tau}} \left[\mathbf{A}_0 \mathbf{Y}_{,t} + \tilde{\mathbf{F}}_{i,i}^{adv}(\mathbf{Y}) - \tilde{\mathbf{F}}_{i,i}^{diff}(\mathbf{Y}) - \tilde{\boldsymbol{\mathcal{F}}} \right] \right\} \mathrm{d}\Omega^e \\ &= \oint_{\Gamma} \left\{ \mathbf{W} \cdot \left[\mathbf{F}_i^{diff}(\mathbf{V}) \cdot \mathbf{n}_i \right] \right\} \mathrm{d}\Gamma \end{aligned} \tag{31}$$

Using the quasi-linear notation, the variational formulation (26) is replaced by the following variational formulation:

$$\begin{aligned} &\int_{\mathbf{\Omega}} \left\{ \mathbf{W} \cdot \left[\mathbf{A}_0 \mathbf{Y}_{,t} + \tilde{\mathbf{A}}_i \mathbf{Y}_{,i} - \tilde{\boldsymbol{\mathcal{F}}} \right] + \mathbf{W}_{,i} \cdot \left[\tilde{\mathbf{K}}_{ij} \mathbf{Y}_{,j} \right] \right\} \mathrm{d}\mathbf{\Omega} \\ &+ \sum_e \int_{\Omega^e} \left\{ \left(\tilde{\mathbf{A}}_i^t \cdot \mathbf{W}_{,i} \right) \underline{\tilde{\tau}} \left[\mathbf{A}_0 \mathbf{Y}_{,t} + \tilde{\mathbf{A}}_i \mathbf{Y}_{,i} - \left(\tilde{\mathbf{K}}_{ij} \mathbf{Y}_{,j} \right)_{,i} - \tilde{\boldsymbol{\mathcal{F}}} \right] \right\} \mathrm{d}\Omega^e \\ &= \oint_{\Gamma} \left\{ \mathbf{W} \cdot \left[\left(\tilde{\mathbf{K}}_{ij} \mathbf{Y}_{,j} \right) \cdot \mathbf{n}_i \right] \right\} \mathrm{d}\Gamma \end{aligned} \tag{32}$$

Using the matrix of change of variables $\mathbf{A}_0$ and the matrix of stabilization $\underline{\tau}$ of the conservative form in conservative variables, we obtain a general matrix of stabilization $\underline{\tilde{\tau}}$ for any type of independent variables $\mathbf{Y}$, so we write $\underline{\tilde{\tau}}$ as follows:

$$\underline{\tilde{\tau}} = \mathbf{A}_0^{-1} \left[\sum_i \left| c_{ij} \mathbf{A}_j \right| \right]^{-1} \zeta(Pe) = \mathbf{A}_0^{-1} \, \underline{\tau} \tag{33}$$

By the means of this study we confirm that, in the case of the flows with dominant advection, the developed Petrov-Galerkin finite element method has really eliminated the non-physical oscillations contrary to the Galerkin's standard finite element method.

III.2. Temporal discretization

The temporal derivatives are approximated using the implicit schema of Euler or the implicit schema of the second order of Gear. The temporal derivative of any quantity $\mathbf{v}(t)$, using the Euler scheme, is given by:

$$\frac{\partial \mathbf{v}}{\partial t} \approx \frac{\mathbf{v}(t + \Delta t) - \mathbf{v}(t)}{\Delta t} \tag{34}$$

with Δt is the time step. The temporal derivative of any quantity $\mathbf{v}(t)$, using the Gear scheme, is given by:

$$\frac{\partial \mathbf{v}}{\partial t} \approx \frac{3\mathbf{v}(t + \Delta t) - 4\mathbf{v}(t) + \mathbf{v}(t - \Delta t)}{2\Delta t} \tag{35}$$

This schema with two time steps, requires a starting procedure, we set $\mathbf{v}(-1) = \mathbf{v}(0)$ when the time $t = 0$, which corresponds to the implicit Euler scheme with the time step $\frac{2}{3}\Delta t$.

III.3. Choice of the element

To solve the viscous compressible flow equations, the triangular element is best adapted. Geometrically, this element provides great flexibility to model the contours of complex geometric shapes. Numerically, the choice of this element imposes conditions on the degree of the interpolation functions. To solve this problem, we have chosen a triangular element for which the components of velocity and momentum per unit volume are approximated by continuous polynomials of the second degree, while the other variables are approximated by continuous linear polynomials. This choice of mixed polynomial approximations makes it possible to verify the stability of the element, and to satisfy the "Inf-Sup" condition [25, 26].

III.4. Method of resolution

The matrix system obtained after the space and time discretization is given by:

$$[\mathbf{M}]\left\{\mathbf{Y}_{,t}\right\} + [\mathbf{K}(\mathbf{Y})]\{\mathbf{Y}\} = \{\mathbf{F}\} \tag{36}$$

where $[\mathbf{M}]$ is the total mass matrix, $[\mathbf{K}(\mathbf{Y})]$ is the global stiffness matrix, $\{\mathbf{Y}\}$ is the global vector of unknown variables, and $\{\mathbf{F}\}$ is the global source vector. The matrix system contains several types of nonlinearities. Nonlinearities that represent the effects of viscosity and compressibility. The additional nonlinearities, if we use the Petrov-Galerkin method of stabilization. Thus, the matrix which results from the system is a hollow, non-linear, non-symmetric and large matrix. This therefore encourages the use of a robust iterative resolution method. In this work we use the Generalized Minimal RESidual (GMRES) iteration method [27, 28, 35]. We conclude that this method is robust, and is specially adapted for solving nonlinear problems.

IV. Numerical simulations

IV.1. Flows around the profile NACA0012

Transonic flow around the NACA0012 profile presenting various difficulties has been resolved using the stabilization methods described previously. The characteristics of these flows vary between 500 and $100\,000$ for the Reynolds number with a Mach number equal to $0,85$. The NACA0012 profile is symmetrical and the coordinates of the upper surface are given by:

$$y(x) = 5t\left(0{,}2969x^{1/2} - 0{,}126x - 0{,}3516x^2 + 0{,}2848x^3 - 0{,}1015x^4\right)$$

where x is the distance along the chord from the leading edge ($x = 0$), y is the ordinate on the intrados and t ($= 0{,}12$) is the relative thickness of the profile. The mesh used is composed of $8\,150$ triangular elements. This mesh is refined around the profile, in areas of circulation, in areas of wake and in the areas of the leading edge. Figures 1 shows the geometry of the profile and the flow domain (Figure 1a), the mesh (Figure 1b) with an enlargement around the profile (Figure 1c).

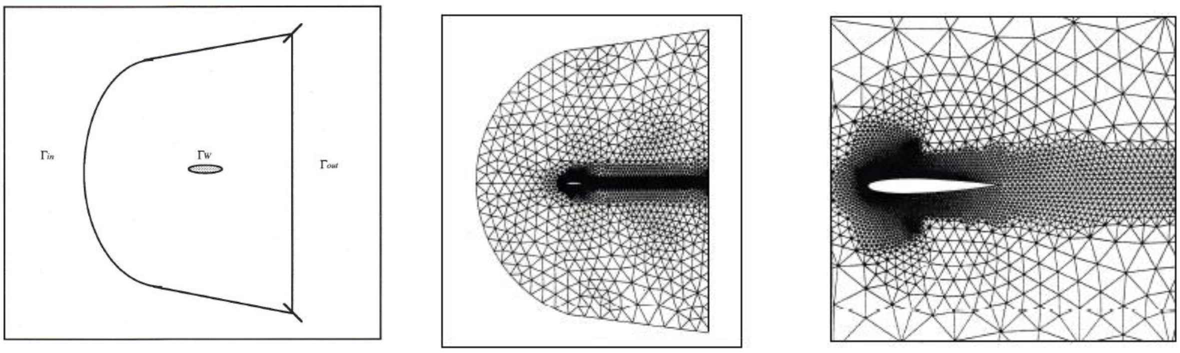

a) Geometry - flow domain *b) Mesh* *c) zoom around the profile*

Figure 1: Geometry of the NACA0012 profile and mesh

At upstream infinity Γ_{in}, the boundary conditions are of Dirichlet type:

$$\begin{cases} Ma_\infty = 0{,}85 \\ \rho = \rho_\infty \\ U_1 = U_\infty \\ U_2 = 0{,}0 \\ E = E_\infty \end{cases} \quad \text{or} \quad \begin{cases} Ma_\infty = 0{,}85 \\ p = p_\infty \\ U_1 = U_\infty \\ U_2 = 0{,}0 \\ T = T_\infty \end{cases}$$

At downstream infinity Γ_{out}, one imposes a boundary condition of Dirichlet: either $p = p_\infty$, or $\rho = \rho_\infty$ dependently of the type of formulation, and the condition $(\underline{\sigma} \cdot n)_1 = 0$. On the wall of the profile Γ_w, one imposes the condition of adherence $\mathbf{U} = 0$. The initial solution used is a uniform field, except for the wall of the profile where the condition is imposed $\mathbf{U} = 0$. For both types of independent variables, three types of flows are solved under the same conditions.

Flow 1: $Re = 10\,000,\ Ma = 0{,}85$

We are in the presence of a weakly turbulent and relatively complex flow. To perform this simulation, the Petrov-Galerkin method is used at the beginning of the resolution. The Reynolds number was increased gradually, by interval of 200. This resolution strategy was exactly applied in the same way for the two types of forms: the conservative form in conservative variables and the conservative form in pseudo-primitive variables. The Mach number contour, density contour and velocity field are shown in figure 2 for the conservative form in conservative variables and in figure 3 for the conservative form in pseudo-primitive variables.

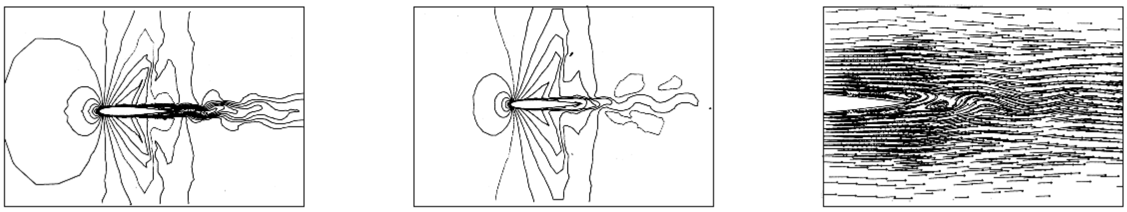

a) Mach number contour *b) Density contour* *c) Velocity field*

Figure 2: Conservative form in conservative variables $\boldsymbol{Re = 10\,000}$

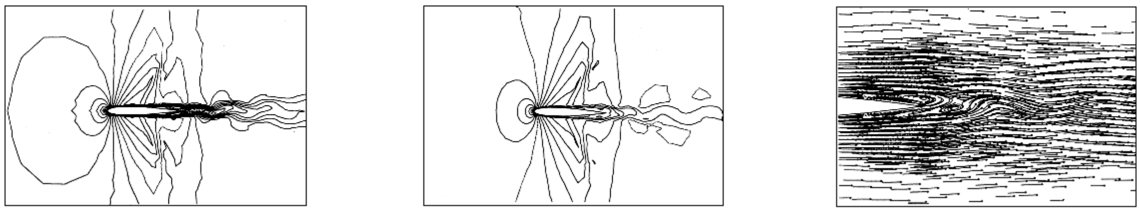

a) Mach number contour *b) Density contour* *c) Velocity field*

Figure 3: Conservative form in pseudo-primitive variables $\boldsymbol{Re = 10\,000}$

In particular, we observe the impact effect of the shock, which is formed around 70% of the chord of the profile but undergoes a pulsation of the boundary layer. The pulsation effect is particularly visible on curves C_p, figure 4.

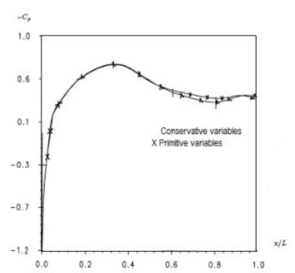

Figure 4: Pressure coefficient

Note also the presence of supersonic pockets in the wake. At a given time step, on the velocity fields (figures 2c and 3c), we distinguish well the stall of vortices.

Flow 2 : $Re = 50\,000, \quad Ma = 0.85$

The purpose of these simulations is to compare the two types of variables. In order to observe the evolution of the simulations, the final result is obtained following a progressive increase of the Reynolds number. The Mach number contour, density contour and velocity field are presented in figure 5 for the conservative form in conservative variables and in the figure 6 for the conservative form in pseudo-primitive variables.

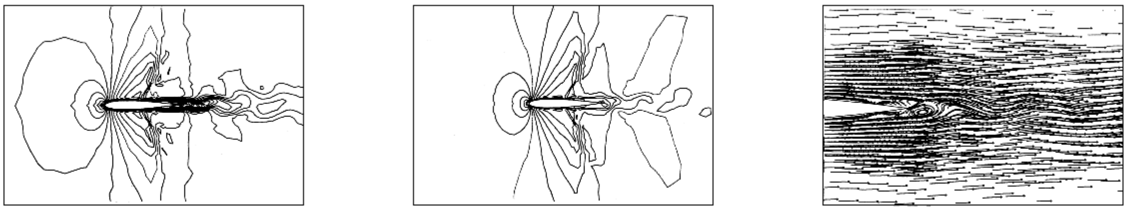

a) Mach contour *b) Density contour* *c) Velocity field*

Figure 5: Conservative form in conservative variables $\boldsymbol{Re = 50\ 000}$

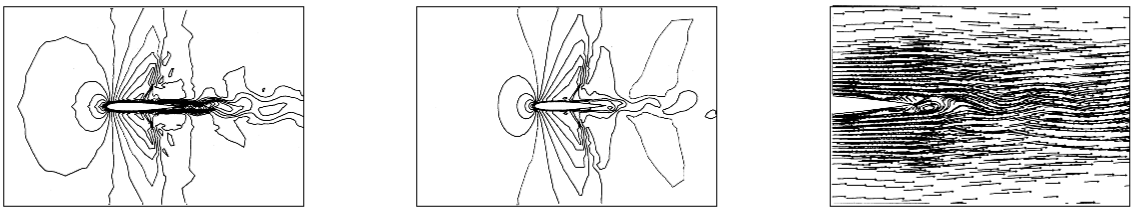

a) Mach contour *b) Density contour* *c) Velocity field*

Figure 6: Conservative form in pseudo-primitive variables $\boldsymbol{Re = 50\ 000}$

From these results, we note that:
- The physical phenomena observed in the case of the preceding simulations ($Re = 10\ 000$) are more apparent and better defined for the two types of variables.
- The phenomenon of shift of the shock wave and the stationary state of the flow.
- The movement of the shock downstream, an elevation of the Mach number in the supersonic zone and the presence of supersonic zones in the wake.
- The phenomenon of stalling alternating swirls with unsteady wake are more apparent on the velocity fields, if one makes a comparison with the case of the previous simulations ($Re = 10\ 000$).

For these simulations, there are really no differences between the two types of variables; but a particular attention on the quality of the results allows us to conclude that the conservative form in pseudo-primitive variables always gives better solutions.

Flow 3: $Re = 100\ 000$, $Ma = 0{,}85$

Keeping the same resolution strategy as the case of previous simulations, i.e. we gradually increase the Reynolds number up to 100 000. At this value of the Reynolds number, we notice that the numerical solution becomes unstable and the results are generally not favorable. For both types of variables, conservative and pseudo-primitive variables, the Mach number contour, density contour and velocity field are shown in Figures 8 and 9. We note the presence of strong oscillations and a deterioration of the Mach number contour. In order to improve the numerical results, it would be better to refine the mesh, or even to use a model of turbulence.

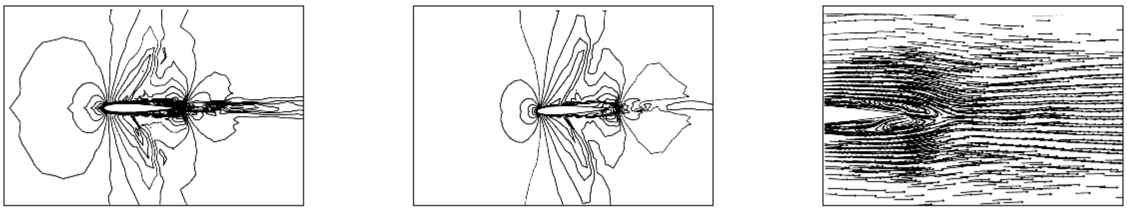

a) Mach number contour b) Density contour c) velocity field

Figure 8: Conservative form in conservative variables $\boldsymbol{Re = 100\ 000}$

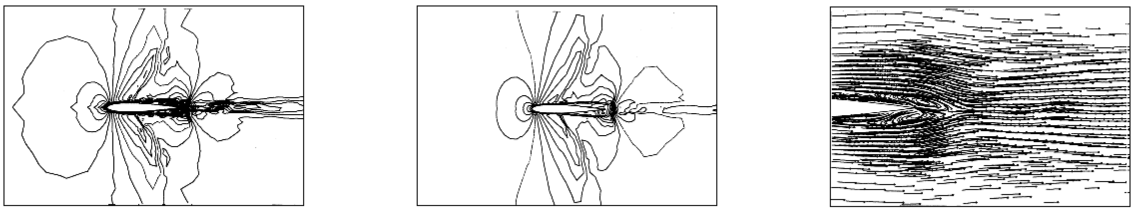

a) Mach number contour *b) Density contour* *c) velocity field*

Figure 9: Conservative form in pseudo-primitive variables $\boldsymbol{Re = 100\ 000}$

IV.2. Supersonic flow on a flat plate

These simulations show a supersonic flow, at Mach 3, along a flat plate. The computation domain is a rectangle of length 1,6 on the $x - axis$ and width 1 on the $y - axis$. The numerical solutions are obtained on a structured mesh, composed of 2 560 triangular elements and 5 265 nodes, illustrated in figure 10.

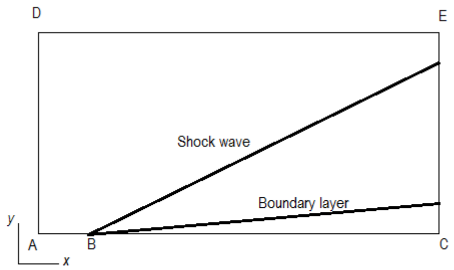

Figure 10: Geometry - Computation domain

At the inlet of the flow [AD] and at the upper boundary of the domain [DE], all the variables are fixed at their values at infinity. At the exit of the domain, border] EC [, all the variables are left free. On the boundary of the domain] AB [, we impose the horizontal component of the momentum per unit of volume at zero, $\mathbf{U}_2 = 0$. On the flat plate, boundary of the domain [BC], one imposes the condition of adhesion $\mathbf{U} = 0$ and the condition of adiabaticity through the temperature:

$$T = T_{stag} = T_\infty \left(1 + \frac{\gamma - 1}{2} M_\infty^2\right)$$

The initial solution used is a uniform field, except on the plane plate [BC] where the normal and tangential components of the momentum per unit volume are imposed equal to zero. The resolution strategy is to set the Reynolds number to 1 000 and then 10 000 and the Mach number to 3, using the Petrov-Galerkin method from the beginning. The step in time is performed with local time steps, $CFL = 0{,}5$. As expected, under these physical and numerical conditions, the numerical results clearly show the presence of the boundary layer and oblique shock. These physical phenomena are clearly visible on the density contour, the Mach number contour and the pressure contour, for both formulations. The contours are shown in figures 11 and 12 for the Reynolds number equal to 1 000 and in figures 13 and 14 for the Reynolds number equal to 10 000. For numerical simulations with Reynolds number equal to 1000, the conservative form in pseudo-primitive variables gives a better quality solution, it presents less oscillations. In figure 15, the pressure coefficient is compared with that obtained by [28] using a finite element method and entropy variables.

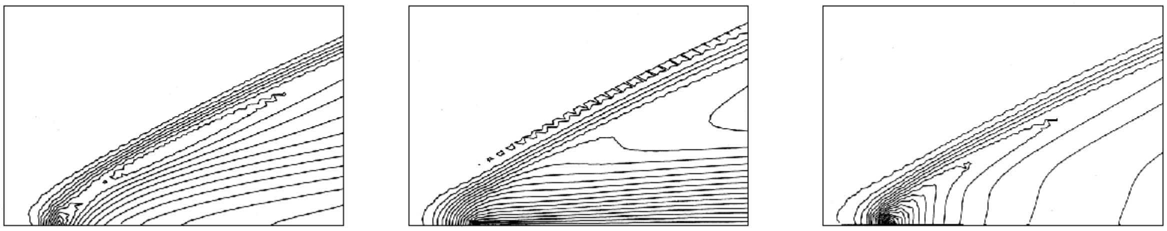

a) Density contour *b) Mach number contour* *c) Pressure contour*

Figure 11: Conservative form in conservative variables $\boldsymbol{Re = 1\,000,\quad Ma = 3}$

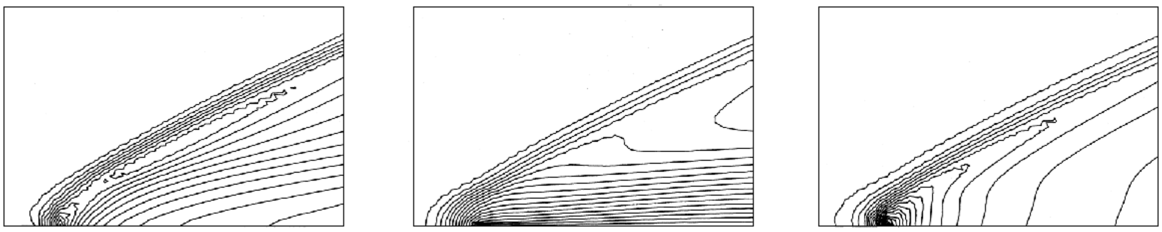

a) Density contour *b) Mach number contour* *c) Pressure contour*

Figure 12: Conservative form in pseudo-primitive variables $\boldsymbol{Re = 1\,000,\quad Ma = 3}$

For numerical simulations with Reynolds number equal to 10,000, conservative form in conservative variables shows remarkable oscillations, especially for Mach number contour; which is not the case for the conservative form in pseudo-primitive variables. In figure 15b, the pressure coefficients for both forms are illustrated for the Reynolds number equal to 10 000.

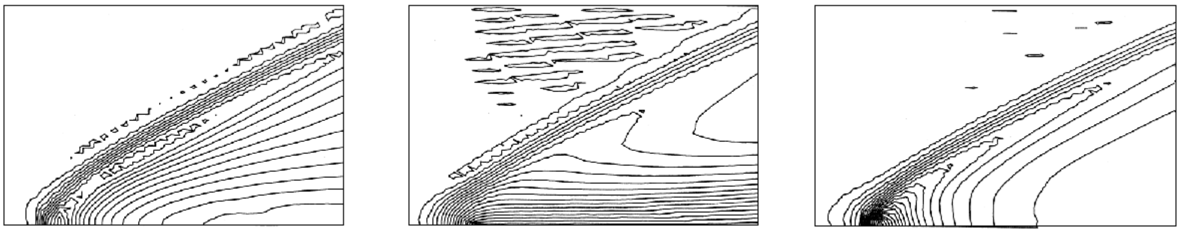

a) Density contour *b) Density contour* *c) Pressure contour*

Figure 13: conservative form in conservative variables $\boldsymbol{Re = 10\,000,\quad Ma = 3}$

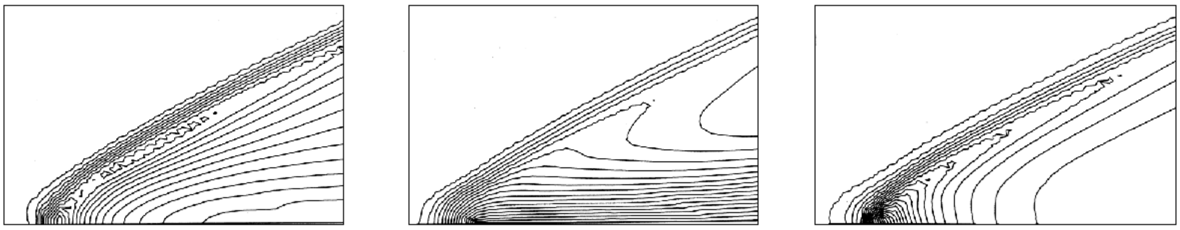

a) Density contour *b) Density contour* *c) Pressure contour*

Figure 14: conservative form in pseudo-primitive variables $\boldsymbol{Re = 10\,000,\quad Ma = 3}$

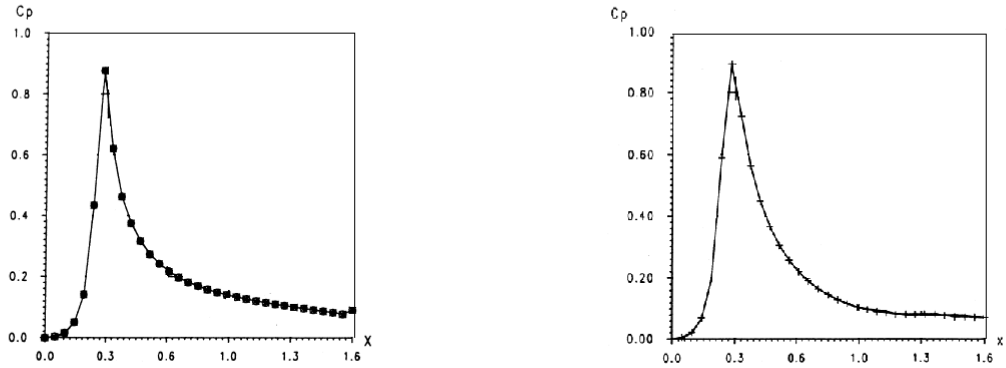

a) $Re = 1\,000$ *a)* $Re = 10\,000$

Figure 15: Pressure coefficients

V. Conclusion

We have developed a finite element method for the simulation of viscous compressible flows. The equations, which describe these viscous compressible flows of a perfect and Newtonian fluid, are written in conservative form. From the study of the physical and numerical behaviour of the two types of independent variables, we conclude that: the numerical results obtained by the pseudo-primitive variables are of a better quality compared to the numerical results obtained by the conservative variables. In addition, the use of pseudo-primitive variables makes it easy to apply physical boundary conditions. An identical approximation for all variables reveals oscillations in the fields of density and pressure. This problem of instability has been solved by the choice of triangular elements, for which: the components of velocity and momentum per unit of volume are approximated by continuous polynomials of the second degree, whereas the other variables are approximated by continuous linear polynomials. This choice of mixed polynomial approximations satisfies the stability condition "Inf-Sup". Spatial discretization by the finite element method with Galerkin-type weighting leads to nonphysical oscillations, when advection dominates. In order to obtain stable results, a variant of the Petrov-Galerkin method has been developed and used successfully. The success of such a method is based on the constitution of the stabilization matrix. We proposed a definition of the stabilization matrix for the conservative form in conservative variables. Starting from this definition, we have derived a general form of this matrix for all types of independent variables. The matrix system obtained, after the spatial and temporal discretization, comprises several types of nonlinearities. To solve this matrix system, we successfully used a variant of the iterative algorithm GMRES with diagonal pre-conditioning. Diagonal pre-conditioning is simple and effective. The numerical methods and techniques developed have been successfully validated on several situations of compressible viscous flows.

References

[1] Elkadri E. Nacer E., 1992. Modélisation des écoulements compressibles visqueux par la méthode des éléments finis, *Mémoire de maîtrise, Département de génie mécanique, Université Laval, Québec, Canada*.

[2] Elkadri E. Nacer E., 1995. Une méthode d'éléments finis pour la dynamique des gaz et conception orientée objet du code de calcul. *Ph.D., Thèse de doctorat, Département de génie mécanique, Université Laval, Québec, Canada.*

[3] Hansbo P. and Johnson C., 1991. Adaptive streamline diffusion methods for compressible flow using conservative variables. *Computer Methods in Applied Mechanics and Engineering*, Vol. 87, pp. 267-280.

[4] Hansbo P., 1993. Explicit streamline diffusion finite element methods for the compressible Euler equations in conservation variables. *Journal of Computational Physics*, Vol. 109, No 2, pp. 274-288.

[5] Hughes T.J.R., Franca L.P. and Mallet M., 1986. A new finite element formulation for computational fluid dynamic: I. Symmetric forms of the compressible Euler and Navier-Stokes equations and the second law of the thermodynamics. *Computer Methods in Applied Mechanics and Engineering*, Vol. 54, pp. 223-234.

[6] Boivin S. 1990. Simulation d'écoulements compressibles à nombre de Reynolds élevé. *Thèse de doctorat (Ph.D.), Université Laval, Québec, Canada*.

[7] Fortin M., Manouzi H. and Soulaimani A., 1993. On finite element Approximations and stabilization method for compressible viscous Flows. *International Journal For Numerical Methods in Fluids*, Vol. 17, pp. 477-499.

[8] Codina R., 1998. Comparison of some finite element methods for solving the diffusion–convection–reaction equation. *Computer Methods in Applied Mechanics and Engineering*, Vol. 156, pp. 185-210.

[9] Brooks A.N. and Hughes T.J.R., 1982. Streamline upwind Petrov-Galerkin formulation for convection dominated flows with particular emphasis on the incompressible Euler and Navier-Stokes equations. *Computer Methods in Applied Mechanics and Engineering*, Vol. 32, pp. 199-259.

[10] Burman E., 2010. Consistent SUPG-method for transient transport problems: Stability and convergence, *Computer Methods in Applied Mechanics and Engineering*, Vol. 199, pp. 1114-1123.

[11] John V. and Novo J., 2011. Error analysis of the SUPG finite element discretization of evolutionary convection-diffusion-reaction equations. *SIAM Journal on Numerical Analysis*, Vol. 49, No 3, pp. 1149-1176.

[12] Ganesan S., 2012. An operator-splitting Galerkin/SUPG finite element method for population balance equations: Stability and convergence. *ESAIM: Mathematical Modeling and Numerical Analysis (M2AN)*, Vol. 46, pp. 1447-1465.

[13] Hughes T.J.R., Scovazzi G. and Tezduyar T.E., 2010. Stabilized methods for compressible flows. *Journal of Scientific Computing*, Vol. 43, pp. 343-368.

[14] Hughes T.J.R., Franca L.P. and Hulbert G.M., 1989. A new finite element formulation for computational fluid dynamics: VIII. The Galerkin/least-squares method for advective-diffusive equations. *Computer Methods in Applied Mechanics and Engineering*, Vol. 73, 173-189.

[15] Burman E. and Hansbo P., 2004. Edge stabilization for Galerkin approximations of convection-diffusion-reaction problems. *Computer Methods in Applied Mechanics and Engineering*, Vol. 193, pp. 1437-1453.

[16] Burman E., Fernandez M. and Hansbo P., 2006. Continuous interior penalty finite element method for Oseen's equations. *SIAM Journal on Numerical Analysis*, Vol. 44, pp. 1248-1274.

[17] Ganesan S. and Tobiska L., 2010. Stabilization by local projection for convection-diffusion and incompressible flow problems. *Journal of Scientific Computing*, Vol. 43, pp. 326-342.

[18] Codina R., 2000. Stabilization of incompressibility and convection through orthogonal sub-scales in finite element methods. *Computer Methods in Applied Mechanics and Engineering*, Vol. 190, pp. 1579-1599.

[19] Bazilevs Y. and Akkerman I., 2010. Large eddy simulation of turbulent Taylor–Couette flow using isogeometric analysis and the residual-based variational multiscale method. *Journal of Computational Physics*, Vol. 229, pp. 3402-3414.

[20] Hughes T.J.R., Feijóo G.R., L. Mazzei and Quincy J.-B., 1998. The variational multiscale method a paradigm for computational mechanics. *Computer Methods in Applied Mechanics and Engineering*, Vol. 166, pp. 3-24.

[21] Marras S., Kelly J.F., Giraldo F.X. and Vázquez M., 2012. Variational multiscale stabilization of high-order spectral elements for the advection–diffusion equation. *Journal of Computational Physics*, Vol. 231, pp. 7187-7213.

[22] Saad Y. and Schultz M. H., 1986. GMRES : a generalized minimal residual algorithm for solving nonsymmetric linear systems. *SIAM J. Sci, Statist. Comput, Vol. 7 (3), pp. 856-869.*

[23] de Frutos J., B. Garcia-Archilla, V. John and J. Novo, 2014. An adaptive SUPG method for evolutionary convection–diffusion equations, *Computer Methods in Applied Mechanics and Engineering*, Vol. 273, pp. 219-237.

[24] John V. and Schmeyer E., 2008. Finite element methods for time-dependent convection-diffusion-reaction equations with small diffusion. *Computer Methods in Applied Mechanics and Engineering*, Vol. 198, pp. 475-494.

[25] Babuska I., 1971. Error-bounds for finite element method. *Numerische Mathematik.* Vol. 16, pp. 322-333.

[26] Brezzi F., 1974. On the existence uniqueness and approximation of salddle-point problems arising from lagrangian multipliers. *ESAIM: Mathematical Modelling and Numerical Analysis*, Vol. 8, pp.129-151.

[27] Roos H.G., Stynes M. and Tobiska L., 2008. Numerical Methods for Singularly Perturbed Differential Equations, *Springer Series in Computational Mathematics*.

[28] Shakib F., Hughes T.J.R. and Johan Z., 1989. A multi group preconditioned GMRES algorithm for non symmetric systems arising in finite element analysis. *Computer Methods in Applied Mechanics and Engineering*, Vol. 75, pp. 415-465.

[29] Whiting C.H., Jansen K.E. and Dey S., 2003. Hierarchical basis for stabilized finite element methods for compressible flows. *Computer Methods in Applied Mechanics and Engineering*, Vol. 192, pp. 5167-5185.

[30] Whiting C.H. and Jansen K.E., 2001. A stabilized finite element method for the incompressible Navier-Stokes equations using a hierarchical basis. *International Journal for Numerical Methods in Fluids*, Vol. 35, pp. 93-116.

[31] Elkadri E. N. E., Soulaïmani A., Deschênes C., 2000. A finite element formulation of compressible flows using various sets of independent variables. *Computer Methods in Applied Mechanics and Engineering*, Vol. 181, pp. 161-189.

[32] Rebaine Ali, Soulaïmani Azzeddine, Mercadier Yves et Elkadri Elyamani Nacer-Eddine, 1997. Une méthode d'éléments finis pour les écoulements internes compressibles: application aux éjecteurs. *Revue Européenne des Éléments Finis*, Vol. 6, No 5-6/1997, pp. 545-587.

[33] Soulaïmani Azzeddine, Elkadri Elyamani Nacer-Eddine, Deschênes Claire, 1994. Une méthode d'éléments finis pour le calcul des écoulements compressibles utilisant les variables conservatives et la méthode SUPG. *Revue Européenne des Éléments Finis.* Vol. 3, No 2/1994, pp. 211-245.

[34] Soulaïmani Azzeddine et Elkadri Elyamani Nacer-Eddine, 1992. Sur une méthode de décentrage de schémas d'éléments finis résolvant les équations de Navier-Stokes et de Saint-Venant. *Revue Européenne des Éléments Finis,* Vol. 1, No 3/1992, pp. 279-307.

[35] Saad Y., 1994. ILUT a dual threshold incomplete ILU factorization, *Numerical Linear Algebra with Applications,* Vol. 1, pp. 387-402.

Nacer E. EL KADRI E "Numerical simulation of compressible viscous flow.” IOSR Journal of Mechanical and Civil Engineering (IOSR-JMCE) , vol. 15, no. 1, 2018, pp. 44-56